

Correlated hopping through thin disordered insulators

D. Ephron and M. R. Beasley

Department of Applied Physics, Stanford University, Stanford, California 94305

H. Bahlouli* and K. A. Matveev†

Theoretical Physics Institute, University of Minnesota, Minneapolis, Minnesota 55455

(Received 4 October 1993)

We present data from Mo/*a*-Si/Mo tunnel junctions together with calculations that show that hopping transport via localized states in amorphous silicon is highly correlated. Localized states whose single-particle energies lie well below the Fermi level participate in transport due to the large on-site Coulomb interaction U . The results also imply that the density of these states is roughly constant over a wide energy range of order U .

Electron-electron interactions are believed to play an important role in transport through disordered insulators with a high density of localized states. Efros and Shklovskii predicted that the Coulomb interactions between electrons on different sites in a system exhibiting Mott variable range hopping (VRH) should lead to a gap in the density of states at sufficiently low temperature and to a crossover from the Mott $T^{-1/4}$ law to a $T^{-1/2}$ law.¹ The experimental evidence from many different systems strongly indicates the presence of this crossover.² Little attention has been paid, however, to the role of the *on-site* Coulomb interaction in hopping transport. Glazman and Matveev predicted that in a tunnel junction with a thin disordered insulating barrier, the on-site Coulomb interaction would lead to correlated resonant tunneling via localized states, which would reveal itself in the magnetic-field dependence of the conductance.³ Two of us (D.E. and M.R.B) have recently demonstrated this effect experimentally using deposited amorphous silicon (*a*-Si) tunnel barriers, but were led to postulate correlations in the hopping transport channels incorporating two localized states in order to account fully for the data.⁴

In this paper, we confirm the correlated nature of both the resonant and the multisite hopping channels and present theoretical calculations in quantitative agreement with the data. In addition, our results demonstrate that because of the correlated nature of the transport, localized states far below the Fermi energy can participate in transport in disordered insulators, in contrast to the usual single-particle picture. Finally, we note the implications of these results for the magnetoresistance in the variable-range-hopping regime.

To understand the physics of these correlations, consider resonant tunneling through a single site near the Fermi level and situated in the center of the barrier for simplicity. In the absence of any Coulomb interactions, the two spin-degenerate localized states associated with the single site support two independent resonant conduction channels. If U is much greater than both eV and kT , however, then these two channels become highly correlated. While an electron is tunneling through one of the

two localized states, its wave function is highly peaked around the site, thus raising the energy of the second state by U above its single-particle value and preventing a second electron from tunneling via the other channel simultaneously [Fig. 1(a)]. The effective number of channels through a single localized site will always fall between one and two [represented schematically by one solid and one dashed line in Fig. 1(a)]. The exact degree of correlation for a given site depends upon the fraction of the time that it is occupied, which is in turn a function of the ratio of the coupling energies to each of the two electrodes and also of the single-particle energy of the states.

The Coulomb correlations also lead to a novel effect: localized sites with single-particle energies close to $\epsilon_F - U$ can participate in resonant transport [Fig. 1(b)]. One of the two states on each such site will always be occupied, since the energy to add the first electron is well below the Fermi level. The addition of a second electron from the

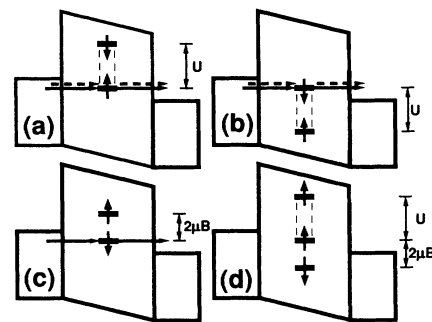


FIG. 1. Schematic representation of correlated resonant tunneling via localized states. A large on-site Coulomb energy U allows only one electron to tunnel through a given site at a time (a), but also enables electrons to tunnel through sites found roughly U below the Fermi level (b); the number of effective channels is between 1 and 2, indicated by the solid plus dashed line. For type-A states in a strong magnetic field, spin-down electrons can tunnel through uncorrelated channels (c), while spin-up electrons (spin parallel to the field) are completely blocked (d).

Fermi level is elastic, allowing resonant tunneling through the site. We denote sites whose single-particle energy level is near the Fermi level as “type *A*” and those nearly U below the Fermi level as “type *B*.” Type-*B* sites manifest the same correlations as type-*A* sites, as is easily seen by considering holes tunneling through them in the reverse direction: a hole tunneling via a type-*B* state blocks the second channel associated with the same site, since two holes cannot occupy a type-*B* site simultaneously. Electron-hole symmetry requires that a type-*B* site yield the same contribution to the conductance as a type-*A* site at the same location with $\varepsilon_A = -\varepsilon_B - U$ and the applied bias reversed.

The application of a strong magnetic field ($U \gg \mu_B B \gg kT \gg eV$) clearly reveals the correlation effects. The field lifts the degeneracy of the two spin states associated with each localized site, with the result that all of the resonant tunneling proceeds through uncorrelated channels. Figures 1(c) and 1(d) illustrate the effect of a strong field on conduction through type-*A* sites. Since $\mu_B B \gg kT$ and eV , the field pushes all of the states that contribute to the transport in zero field so far from the Fermi level that they no longer contribute to the conduction. In our *a*-Si junctions, the density of localized states is sufficiently high [$g \approx 5 \times 10^{18} \text{ eV}^{-1} \text{ cm}^{-3}$ (Ref. 5)] that, on average, a spin-down state pushed down from above [Fig. 1(c)] and a spin-up state pushed up from below [Fig. 1(d)] replace every pair of degenerate states that contribute to the conduction in zero field. These replacement states reside on different sites and are uncorrelated with one another.

Due to the spin correlations, however, the configuration depicted in Fig. 1(d) does not contribute to the conduction since the spin-down state associated with the same site as the spin-up state near the Fermi level will always be occupied, thus changing the energy needed to add a spin-up electron to $\varepsilon_F + U$ and thereby blocking resonant tunneling. Type-*B* sites exhibit analogous correlations. In conclusion, in a strong field, a single uncorrelated resonant channel replaces every pair of correlated resonant channels found in zero field. Thus, the ratio of the conductance of the junction in a strong field to that in zero field directly measures the degree of correlation present in the zero-field transport. Note that the resonant states act as spin polarizers in a strong field: *A* sites allow only spin-down electrons to tunnel [Fig. 1(c)], while *B* sites transport only spin-up electrons.

The effect of a magnetic field on the zero-bias resonant-tunneling conductance, G_R , has been calculated assuming $U \gg kT \gg eV$.³ After averaging over a uniform density of localized states (in energy and space⁶), it is found that $G_R(B)$ obeys a universal dependence on the ratio of the Zeeman splitting of the electronic states to the thermal broadening of the Fermi surfaces in the electrodes, $G_R(B)/G_R(0) = F_R(\mu_B B/kT)$. The function $F_R(x)$ is the solid line in Fig. 2. Note that $r_1 \equiv G_R(\infty)/G_R(0) = (2 \ln 2)^{-1} \approx 0.721$, indicating that on average each correlated state conveys only 70% ($= 0.5/r_1$) of the current of an uncorrelated state. This result is independent of the proportion of type-*A* and type-*B* states present.

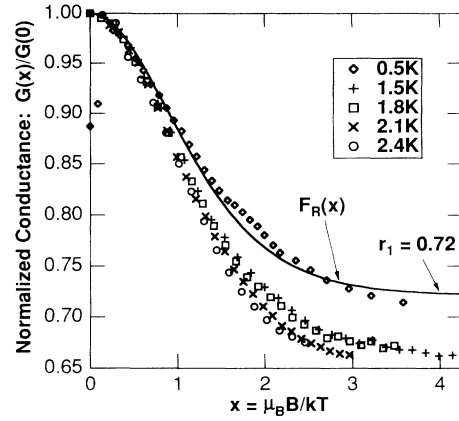


FIG. 2. The normalized magnetic-field dependence of the zero-bias conductance, plotted as a function of the scaling parameter x . The solid line shows the theoretical prediction for resonant tunneling.

Previously, we have reported^{4,5} the details of the techniques used to fabricate and measure the junctions and we have shown that the localization length $\alpha^{-1} = 6.8 \text{ \AA}$. We can then estimate $U \approx e^2/\varepsilon\alpha^{-1} \approx 100 \text{ meV}$. Lattice relaxation will lower this,⁷ but U is clearly much greater than any other energy in our measurement. The data reported in this paper come from three nominally identical samples with barrier thickness $d = 120 \text{ \AA}$, molybdenum electrodes, and an area of $90 \times 90 \mu\text{m}^2$. The direct tunneling contribution to their conductance and the orbital effect of the applied field are both negligible for these samples.^{4,5} Two of the samples were patterned on the same substrate and measured in a pumped He cryostat. They differed in conductance by 1% but showed identical normalized results, which were published previously.⁴ The third sample was deposited simultaneously on a separate substrate and measured in a dilution refrigerator from 100 to 700 mK. The resistance of this sample was 8% greater than the first one, which corresponds to a difference in barrier thickness of about 1 \AA .

Figure 2 shows the zero-bias conductance for five different temperatures as a function of the magnetic field, scaled to $x = \mu_B B/kT$ for each curve. The solid line shows the theoretical prediction for resonant tunneling. There are no adjustable parameters. The ordinate of each curve is normalized to the value of the conductance at that temperature in zero field, except for the 500-mK data, which is normalized to the theoretical curve at $x = 0.1$; below this value, the field is insufficient to quench the superconductivity of the Mo electrodes, accounting for the anomalous first two points.

As argued previously,⁴ the deviation of the higher temperature data from the theoretical curve is due to the non-negligible two-site hopping component of the conductance at these temperatures, ranging from 14% at 1.5 K up to 26% at 2.4 K. The hopping component at 500 mK is less than 4%, so we would expect this data to fall just below the theoretical curve for resonant tunneling at high values of x . The 500-mK curve confirms our earlier attribution of the systematic high-temperature deviations from the theoretical curve to the presence of correlations

in the $n = 2$ hopping channel.

The inset of Fig. 4 schematically depicts the two-site hopping channel. The $L \rightarrow 1$ and $2 \rightarrow R$ transitions are elastic whereas the $1 \rightarrow 2$ hop is inelastic and accompanied by the emission or absorption of a phonon. The zero-bias conductance due to inelastic channels of this type, G_2 , has been calculated and it is found after averaging over a dense distribution of localized states that $G_2(T) = \sigma_2 T^{4/3}$ for $eV \ll kT$.⁸ We have verified this simple power-law behavior as well as the value of the complicated prefactor for a wide variety of barrier thicknesses.⁵ Here we use this understanding to calculate the two-site hopping contribution to the total conductance.

Figure 3 shows the temperature dependence of the zero-bias conductance over a wide temperature range. In fact, the data at low (circles) and high (squares) temperatures are from different samples on different substrates. The low-temperature data have been scaled up by 8% to account for the difference in zero-bias resistance, as explained above. The low-temperature data (circles) were taken in an applied field of about 1 kG to suppress the superconducting gap in the electrodes and represent the average of 13 measurement sweeps to reduce the $1/f$ noise, which increases in severity as the temperature is lowered. The solid line is a fit to the form $G(T) = G_R + \sigma_2 T^m$, with G_R , σ_2 , and m as free parameters. The best fit to the high-temperature data (squares) yields $m = 1.32$, in close agreement with the theoretical prediction of $\frac{4}{3}$. (Note also the circle at 4.2 K.) From the fit, we deduce the fraction of the conductance at each temperature due to resonant tunneling and that due to two-site inelastic hopping.

For the samples studied here, inelastic hopping through three or more sites, which gives rise to terms in the conductance with higher powers of T , becomes appreciable only above 7 K. The deviation from the fit below 450 mK, shown expanded in the inset, is a zero-bias anomaly (ZBA) that has previously been seen in all of the junctions with thinner barriers. The characteristic temperature at which this anomaly appears increases as the barrier is made thinner, thereby preventing measurement

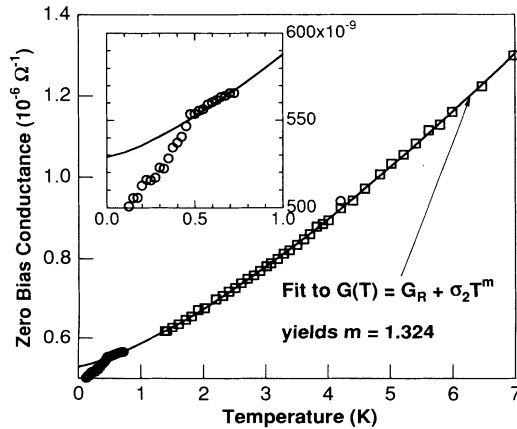


FIG. 3. Temperature dependence of the zero-bias conductance, in excellent agreement (down to 450 mK) with the theory of two-site inelastic hopping, which predicts $m = \frac{4}{3}$. Inset: closeup of the ZBA.

of the Coulomb correlations of the resonant tunneling in thinner samples; we are presently investigating the ZBA.

Now consider the field dependence of the two-site hopping conductance. Figure 4 demonstrates the correlated nature of this inelastic channel. We extract this information by subtracting the resonant part of the transport, $G_R F_R(\mu B/kT)$, from each of the high-temperature curves in Fig. 2 and then renormalizing the curves to their zero-field values. Thus, the curves in Fig. 4 measure the Coulomb correlations through the two-site inelastic chains. Not surprisingly, the correlations are universal in the parameter x , so we can define $F_2(x) = G_2(B, T)/G_2(0, T)$. The deviations at higher x in Fig. 4 are not systematic and, we believe, are merely an amplification of the noise in the data by the subtraction procedure described above. Figure 4 looks qualitatively similar to Fig. 2, but has a different limiting value at large x : the suppression of the conductance is much greater for the hopping channel than for the resonant channel.

In order to understand the implications of this difference, we have calculated the correlations through the inelastic channel using the techniques outlined in Refs. 3 and 8. The calculation is considerably more difficult than for the resonant case, however, because of the necessity of integrating over two spatial coordinates as well as energy, and the need to consider both the on-site and the intersite Coulomb interactions.⁹ Neglecting lattice relaxation effects, the intersite Coulomb correlation energy U_{12} is roughly $U/6$, since the distance between site 1 and site 2 is approximately $6a^{-1}$ for those two-site chains that contribute the most to G_2 . The precise value of U_{12} is not important. There are now eight distinct conducting configurations, denoted as AA , $A'A'$, $A'B''$, $B''A'$, $A''B'$, $B'A''$, $B'B'$, and BB , where the first (second) symbol indicates the approximate single-particle energy of the first (second) localized site in the hopping chain: ϵ_F (type A), $\epsilon_F - U_{12}$ (A'), $\epsilon_F - 2U_{12}$ (A''), $\epsilon_F - U$ (B''), $\epsilon_F - U - U_{12}$ (B'), and $\epsilon_F - U - 2U_{12}$ (B). Because of this complexity, we have so far restricted the calculation to computing $r_2 \equiv F_2(\infty)/F_2(0)$, which contains the important information.

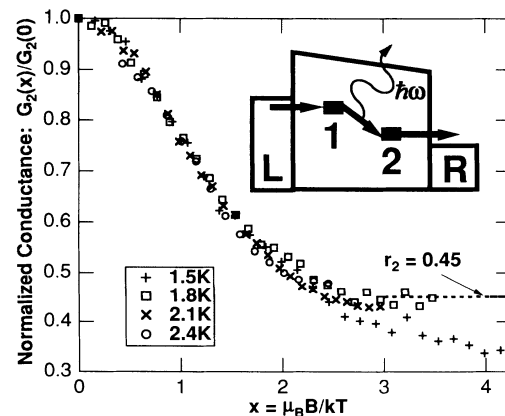


FIG. 4. The scaled magnetic-field dependence of the two-site inelastic hopping conduction. Inset: schematic representation of a two-site inelastic hopping chain (see text).

In contrast to the case of resonant tunneling, the result depends on the relative density of type-*A* and type-*B* states. The *A* series and the *B* series of localized states differ fundamentally in that they act as spin polarizers of opposite polarity for the tunneling electrons in a strong field, as motivated in the discussion of Fig. 1. Thus, the magnetic field completely suppresses the contribution of

the four mixed-type configurations. For $x \gg 1$, only the *AA*, *A'A'*, *BB*, and *B'B'* configurations contribute, albeit with some suppression in analogy to the resonant case: a single uncorrelated hopping channel replaces every pair of correlated hopping channels when $x \gg 1$. The final result of the calculation is

$$r_2 = \frac{3.10[g^2(A) + g^2(A') + g^2(B') + g^2(B)]}{3.85[g^2(A) + g^2(B)] + 3.87[g^2(A') + g^2(B')] + 6.03[g(A')g(B'') + g(A'')g(B')]} ,$$

where $g(A)$ is the density of type-*A* states, etc.

If all of the localized sites contributing to transport were to be found in the range of energies encompassed by the *A* series of energies or the *B* series, but not both, then the calculation predicts $r_2 = 0.8$. If, on the other hand, the density of localized states is taken to be the same at the six energies enumerated above, then $r_2 = 0.45$, in excellent agreement with the experimental results (Fig. 4). If we take the experimental value to be 0.45 ± 0.10 , then we reach the interesting conclusion that the density of states at the six energies are all within a factor of 2 or 3 of one another, barring any pathological dependence of the density of localized states on energy.

The experimental results displayed in Fig. 4 in conjunction with the theoretical calculation outlined above lead to two important conclusions. First, transport via deep defects, which is usually thought of in terms of the localized states *right at* the Fermi level, in fact involves some states whose single-particle energy levels lie very far below the Fermi level; the actual motion of the electrons is highly correlated. To our knowledge, this paper is the first report of the experimental observation of these correlations, which should be present at all temperatures for which transport via localized states is the dominant conduction mechanism. Second, the density of deep defects (dangling bonds) in unhydrogenated amorphous sil-

icon is roughly constant from ϵ_F at least down to $\epsilon_F - U$.

We can extend these conclusions to variable range hopping, where U_{12} will take on a distribution of values, and localized states over a wide continuum of energies will participate in transport. In principle, the magnetoresistance should be enormous for $x \gg 1$, since the type-*A* sites ($\epsilon > \epsilon_F - U$) and the type-*B* sites ($\epsilon < \epsilon_F - U$) can no longer exchange electrons. Thus, the density of states effectively drops by a factor of 2. Since $\sigma_{\text{VRH}} = \sigma_0 \exp[-(T_0/T)^{1/4}]$ with $T_0 \propto 1/g$, this implies a dramatic decrease in the conductivity. We have tried to measure this effect, but unfortunately the resistance of our samples becomes too large to measure at the low temperatures necessary to achieve $x \approx 1$.

Finally, we mention that the techniques outlined in this paper may find application as a kind of crude spectroscopy of the defect states in the technologically important forms of doped hydrogenated amorphous silicon or other amorphous semiconductors.

We would like to acknowledge useful discussions with L. Glazman. The work at Stanford was supported by the Office of Naval Research. D.E. acknowledges the support of NDSEG. The work at Minnesota was supported under NSF Contract No. DMR-9117341.

*Present address: Physics Dept., King Fahd University of Petroleum and Minerals, Dhahran, Saudi Arabia.

†Present address: Dept. of Physics, Massachusetts Institute of Technology, Cambridge, MA 02139.

¹A. L. Efros and B. I. Shklovskii, *J. Phys. C* **8**, L49 (1975); in *Electron-Electron Interactions in Disordered Systems* (North-Holland, Amsterdam, 1985).

²See Ju-Jin Kim and Hu Jong Lee, *Phys. Rev. Lett.* **70**, 2798 (1993), and references therein.

³L. I. Glazman and K. A. Matveev, *Pis'ma Zh. Eksp. Teor. Fiz.* **48**, 403 (1988) [*JETP Lett.* **48**, 445 (1988)].

⁴D. Ephron, Y. Xu, and M. R. Beasley, *Phys. Rev. Lett.* **69**, 3112 (1992).

⁵Y. Xu, A. Matsuda, and M. R. Beasley, *Phys. Rev. B* **42**, 1492 (1990); Y. Zu, Ph.D. thesis, Stanford University, 1992; Y. Xu, D. Ephron, and M. R. Beasley (unpublished).

⁶Actually, the calculation assumes only that the density of localized states does not vary appreciably with energy on the scale of μ_B , which is certainly true in this experiment, since $\mu_B(10 \text{ T}) \approx 0.5 \text{ meV}$.

⁷R. A. Street, *Hydrogenated Amorphous Silicon* (Cambridge University Press, Cambridge, 1991).

⁸L. I. Glazman and K. A. Matveev, *Zh. Eksp. Teor. Fiz.* **94**, 332 (1988) [*Sov. Phys. JETP* **67**, 1276 (1988)].

⁹K. Matveev (unpublished).